International Journal of Pharmaceutics 402 (2010) 146–152

Contents lists available at ScienceDirect

International Journal of Pharmaceutics

journal homepage: www.elsevier.com/locate/ijpharm

Different effects of *l*- and *d*-menthol on the microstructure of ceramide 5/cholesterol/palmitic acid bilayers

Hiroshi Watanabe[a], Yasuko Obata[a,*], Yoshinori Onuki[a], Kenya Ishida[b], Kozo Takayama[a]

[a] *Department of Pharmaceutics, Hoshi University, Ebara 2-4-41, Shinagawa-ku, Tokyo, 142-8501, Japan*
[b] *Takasago International Corporation, Nishiyawata 1-4-11, Hiratsuka-city, Kanagawa, 254-0073, Japan*

ARTICLE INFO

Article history:
Received 27 July 2010
Received in revised form 9 September 2010
Accepted 28 September 2010
Available online 12 October 2010

Keywords:
Lipid bilayers
Stratum corneum
Synchrotron X-ray scattering
Menthol
Ceramide
Optical activity

ABSTRACT

The optical activity of transdermal permeation enhancers is one of the crucial factors for the enhancement of drug permeation via the skin. We investigated the effects of optically active menthols on a lipid bilayer model composed of ceramide 5, cholesterol, and palmitic acid. We first examined the fluidizing effects of *l*- and *d*-menthols on the lipid bilayers. The fluorescence anisotropy and thermodynamic parameters, such as the transition temperature and transition enthalpy, were significantly reduced by treatment with the optically active menthols. The effects of *d*-menthol were stronger than those of *l*-menthol. To discuss further, we also performed a detergent insolubility study and measured wide angle X-ray scattering. The amount of liquid-ordered phase membranes in the bilayers was significantly reduced by treatment with *d*-menthol. Whereas, *l*-menthol did not affected to the liquid-ordered phase membranes. The apparent ratio of orthorhombic hydrocarbon chain packing was substantially reduced by treatment with *l*-menthol. Thus, the distinct effects of optically active menthols on lipid bilayers were clarified: *l*-menthol acts on orthorhombic hydrocarbon chain packing with high selectivity, whereas *d*-menthol has no such specific effect. These findings extend our understanding of the mechanisms by which menthols affect the intercellular lipids in the stratum corneum.

1. Introduction

Transdermal drug delivery systems have potential advantages over oral, injection-based, and intravenous drug administration. These advantages include convenience, noninvasiveness, and the avoidance of first-pass degradation of the drug or its metabolism in the gastrointestinal tract or liver. However, drug permeation via the skin is prevented by the barrier function of the stratum corneum, the outermost layer of the skin and it has possibility that dosage is inaccurately in a part of dosage forms. To date, various techniques have been used to promote transdermal drug permeation, including the use of chemical permeation enhancers (Obata et al., 1993; Nakamura et al., 1996), iontophoresis (Kaliam et al., 2004), and microneedles (Prausnitz, 2004). Among these, the use of permeation enhancers is thought to be the most efficient strategy for convenient and safe transdermal drug delivery systems.

l-Menthol is a well-known and efficient permeation enhancer (Obata et al., 1993; Amit et al., 2002; Mohammed et al., 2007), and can enhance the diffusion and/or partition of a drug in the stratum corneum (Barry, 1991). Although the mechanism responsible for this enhancement effect has not yet been clarified, the fluidizing effect of *l*-menthol on the intercellular lipids in the stratum corneum is thought to be a crucial factor. We previously observed the strong conformational disorder of the intercellular lipids in the stratum corneum caused by treatment with *l*-menthol, using Fourier transform infrared spectroscopy (Obata et al., 2010). dos Anjos et al. also reported that terpenes, including *l*-menthol, disrupted the hydrogen-bond network of the polar head groups in the intercellular lipids of the stratum corneum, in an electron spin resonance spectroscopy study (dos Anjos et al., 2007).

It is exceptionally important to understand the effects of *l*-menthol on the intercellular lipids of the stratum corneum, in order for the development of the effective transdermal drug delivery systems. However, it is very difficult to detect such slight changes in the stratum corneum because of its complex microstructure, composed of various lipids.

A simple intercellular lipid model is a useful substitute for the intercellular lipids in the stratum corneum, because the effect of pharmaceutical additives on the microstructure of the intercellular lipid can be detected with a high sensitivity. Many trials using model membranes have been performed to clarify the structure

Abbreviations: CER, ceramide; CHOL, cholesterol; DRM, detergent-resistant membrane; DSC, differential scanning calorimetry; DPH, 1,6-diphenyl-1,3,5-hexatriene; OD, optical density; PA, palmitic acid; SXRS, synchrotron X-ray scattering; TX-100, Triton X-100; WAXS, wide-angle X-ray scattering.

* Corresponding author. Tel.: +81 3 5498 5783; fax: +81 3 5498 5783.
E-mail address: obata@hoshi.ac.jp (Y. Obata).

0378-5173/$ – see front matter © 2010 Elsevier B.V. All rights reserved.
doi:10.1016/j.ijpharm.2010.09.038

and function of the intercellular lipids in the stratum corneum (Bouwstra et al., 2002; Narishetty and Panchagnula, 2005; dos Anjos and Alonso, 2008; Suhonen et al., 2008; Emmanuella et al., 2009; Watanabe et al., 2009; Groen et al., 2010). Recently, we investigated the membrane properties of lipid bilayers composed of the dominant lipids in the stratum corneum, ceramide 5 (CER5), cholesterol (CHOL), and palmitic acid (PA) (Watanabe et al., 2010). With an analysis using the response surface method incorporating spline interpolation and Kohonen's self-organizing maps, we classified the ternary lipid bilayers into four distinct clusters with similar membrane properties. We further confirmed that the CER5/CHOL/PA (26.5:13.9:59.6 mol%) bilayers, the typical lipid bilayer of cluster 2, has a similar structure to the intrinsic intercellular lipids in the stratum corneum, using synchrotron X-ray scattering (SXRS) measurements (Watanabe et al., 2010). Consequently, we believe that CER5/CHOL/PA bilayers are an efficient substitute for the intercellular lipids of the stratum corneum for estimating the local events in the intercellular lipids induced by administration of the permeation enhancers.

In this study, we investigated the effects of *l*- and *d*-menthols on lipid bilayers. Many substances in the human body, such as proteins and enzymes, are optical isomers, which play important roles in biological and pharmaceutical activities. To date, several groups have focused on the involvement of optical activity in transdermal drug delivery. For example, the skin permeation of the optically active ketoprofen differs (Kommura et al., 1998). Zhang et al. reported that the optical activity of limonene affects the lag time in the transdermal transport of ligustrazine hydrochloride (Zhang et al., 2006). Based on these reports, it is possible that the fluidizing effects of optically active menthols on lipid bilayers will differ. We assessed the structural changes in the lipid bilayers induced by *l*- and *d*-menthols by examining various membrane characteristics.

2. Materials and methods

2.1. Materials

(2S,3R)-2-(2-Hydroxyhexadecanoyl) aminooctadecane-1,3-diol (95%) (CER5) was supplied by Takasago International (Tokyo, Japan). CHOL (99%), PA (99%), *l*- and *d*-menthols (99%), and 1,6-diphenyl-1,3,5-hexatriene (DPH; 98%) were purchased from Sigma-Aldrich (St Louis, MO, USA). Isooctylphenoxypolyethoxyethanol (Triton X-100 (TX-100); 98%) was purchased from GE Healthcare Japan (Tokyo, Japan). All other chemicals used were reagent grade.

2.2. Preparation of lipid bilayers suspension

CER5/CHOL/PA bilayers were prepared as reported previously (Wertz et al., 1986; Wang et al., 2004). The molar ratio of CER5/CHOL/PA was 26.5:13.9:59.6 mol%. This is the typical lipid composition of cluster 2, which has a similar structure to the intercellular lipids in the stratum corneum (Watanabe et al., 2010).

In brief, the designated amounts of lipid dissolved in chloroform/methanol (2:1) were transferred into a flask by pipette, and the solvent was removed by evaporation at room temperature under a stream of nitrogen. This procedure resulted in the formation of a thin lipid film in the inside wall of the flask. Acetate buffer (pH 5.0, 10 ml) was added to the flask, and the lipids were hydrated for 30 min above the phase transition temperature in the water bath. The suspension was sonicated for 5 min above the phase transition temperature. The CER5/CHOL/PA bilayer suspension was prepared at a total lipid concentration of 10 mM and stored at room temperature until it was used in the experiments.

2.3. Fluorescence anisotropy measurements

The CER5/CHOL/PA bilayers were labeled with DPH by the addition of 10 μl of 10 mM DPH stock solution freshly prepared in tetrahydrofuran to 1 ml of the liposome suspension and the subsequent incubation of the mixture at 37 °C for 2 h in the dark to complete the reaction. The menthols were then applied to the bilayers by the addition of 750 μl of *l*- and *d*-menthol in 40% ethanol solution to 1 ml of CER5/CHOL/PA bilayers and the incubation of the sample for 2 h at 37 °C. The menthol concentrations were 10, 20, or 30 mol% relative to the amount of lipid, based on the fact that menthol uptake into the human stratum corneum is about 100 mg/g (Mackay et al., 2001).

The fluorescence anisotropy of DPH in the CER5/CHOL/PA bilayers was measured using a fluorescence spectrophotometer (F-7000; Hitachi High-Technologies Co., Tokyo, Japan) at an excitation wavelength of 351 nm and an emission wavelength of 430 nm. Fluorescence anisotropy was calculated with the following equation:

$$A = \frac{I_0 - G \times I_{90}}{I_0 + 2G \times I_{90}} \quad (1)$$

where A is anisotropy, I_0 and I_{90} are the intensities measured parallel and perpendicular to the polarized exciting light, respectively, and G is the instrumental constant.

2.4. Differential scanning calorimetry (DSC) measurements

The DSC measurements were made with a Thermo plus DSC-8230 (Rigaku Co., Tokyo, Japan), with first heating scans at a rate of 10 °C/min. After treatment with optically active menthols, the CER5/CHOL/PA bilayer suspensions were placed in an aluminum pan (Rigaku Co.). The transition temperatures were determined as the peaks of the endothermic transition peaks.

2.5. Wide angle X-ray scattering (WAXS) measurements

Wide angle X-ray scattering measurements were carried out at the Photon Factory BL15A in the High Energy Accelerator Research Organization (Ibaraki, Japan) and BL40B2 (Structural Biology II Beamline) at SPring-8 (Hyogo, Japan). The wavelength (λ) of the X-ray beam was about 0.151 nm and the sample-to-detector distances were about 160 mm for Photon Factory BL15A and 500 mm for BL40B2 at SPring-8. The reciprocal spacing $S = 1/d = (2/\lambda)\sin(2\theta/2)$ was calibrated from the lattice spacing of a plumbum stearate crystal at room temperature, where 2θ is the scattering angle and d is the lattice distance. A sample cell containing CER5/CHOL/PA bilayers treated with the optically active menthol was sealed with a polyimide film and placed in the sample holder of the X-ray diffractometer. The sample temperature was controlled at 35 °C using a differential scanning calorimeter (FP-99; Mettler-Toledo, Tokyo, Japan). The apparent ratio of the hexagonal and orthorhombic hydrocarbon chain packing ($R_{\mathrm{Hexa/Ortho}}$) was calculated according to the following equation, defined previously (Watanabe et al., 2010):

$$R_{\mathrm{Hexa/Ortho}} = \frac{(S_{2.38} - 2 \times S_{2.70})/3}{S_{2.70}} \quad (2)$$

where $S_{2.38}$ is the integrated intensity of the diffraction peak at $S = 2.38\ \mathrm{nm}^{-1}$, and $S_{2.70}$ is that of the peak at $S = 2.70\ \mathrm{nm}^{-1}$. The denominator indicates the apparent area of orthorhombic hydrocarbon chain packing and the numerator indicates the apparent area of hexagonal hydrocarbon chain packing. $S_{2.70} \times 2$ is the apparent area derived from orthorhombic hydrocarbon chain packing in the area of the diffraction peak at $S = 2.38\ \mathrm{nm}^{-1}$. When hexagonal and orthorhombic hydrocarbon chain packing occur in the CER5/CHOL/PA bilayers in equivalent amounts, the $R_{\mathrm{Hexa/Ortho}}$ value

is 1. Greater $R_{Hexa/Ortho}$ values indicate that hexagonal hydrocarbon chain packing is dominant in the CER5/CHOL/PA bilayers.

2.6. Detergent resistance study

Detergent resistance membranes (DRMs) were extracted according to a previous report, with minor modifications (Wang et al., 2004). After treatment with menthols, 750 μl of a 10% TX-100 aqueous solution was added to 1000 μl of CER5/CHOL/PA bilayer suspension, and the sample was incubated at 25 °C for 2 h. The sample was centrifuged at 15,400 × *g* for 10 min to separate the supernatant and pellet. The pellet of DRMs was collected and resuspended in an equal volume of fresh acetate buffer (pH 5.0). The sample was diluted with acetate buffer (pH 5.0), and the optical density (OD) at 400 nm was measured with a spectrophotometer (Ubest-30; Jasco, Tokyo, Japan). The OD at 400 nm of a freshly prepared CER5/CHOL/PA bilayer suspension was also measured, and this value was used as the initial level. Detergent insolubility was calculated with the following equation:

$$\text{detergent insolubility} = \frac{OD_{400\,nm+TX\text{-}100}}{OD_{400\,nm-TX\text{-}100}} \quad (3)$$

where $OD_{400\,nm+TX\text{-}100}$ and $OD_{400\,nm-TX\text{-}100}$ are the ODs at 400 nm for the DRMs and CER5/CHOL/PA bilayers, respectively.

The lipid composition of the DRMs extracted from intact CER5/CHOL/PA bilayers was quantified with the following method. The amount of CER5 was determined using a high-performance liquid chromatograph (LC-20AT; Shimadzu Co., Tokyo, Japan) equipped with a UV/vis detector (PSD-20A; Shimadzu Co.). Chromatographic separation was accomplished with an ODS column (150 mm × 4.6 mm; YMC Co., Ltd., Kyoto, Japan) at 40 °C. A mobile phase of 50 mM ammonium acetate in methanol solution was eluted at 1 ml/min. The column effluent was detected at 210 nm. The calibration curve for the quantification of CER5 was linear over the range of concentrations of 0.5–5.0 mM with a correlation coefficient of $R^2 = 0.989$. The DRMs were dissolved in 50 mM ammonium acetate in methanol solution and 90 μl of the DRM organic solution was injected. CHOL and PA were determined with the Total Cholesterol E-Test Wako and NEFA C-Test Wako (Wako Pure Chemical industries, Osaka, Japan), respectively.

2.7. Statistical analysis

Each value is expressed as a mean ± S.D. For group comparisons, one-way analysis of variance, Student's *t* test and Dunnett's test were used. *P* values of less than 0.05 were considered significant.

3. Results

3.1. Fluidizing effects of optically active menthols on CER5/CHOL/PA bilayers

The effects of 10 mol% optically active menthols on membrane fluorescence anisotropy at 35 °C are shown in Fig. 1. Treatment with *l*- and *d*-menthol significantly reduced the fluorescence anisotropy values, indicating the fluidization of the CER5/CHOL/PA bilayers. Treatment with *d*-menthol induced an especially pronounced, dose-dependent reduction in the fluorescence anisotropy value. This reduction represents the fluidization of the CER5/CHOL/PA bilayers.

Fig. 2 shows the thermograms derived from the DSC measurements. The CER5/CHOL/PA bilayers displayed two endothermic phase transitions near 58.6 °C (first phase transition) and 65.8 °C (second phase transition; Fig. 2(a)). The transition enthalpies of the first and second phase transitions were 2.85 and 4.89 mJ/mg, respectively. Fig. 3 shows the thermotropic properties calculated

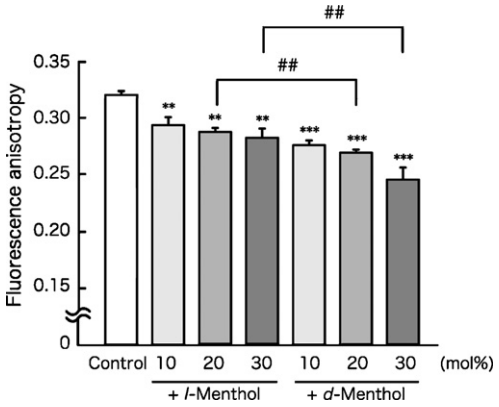

Fig. 1. Fluorescence anisotropy of the DPH in CER5/CHOL/PA bilayers at 35 °C. Each column represents a mean ± S.D. ($n = 3$). $^{**}P < 0.01$ and $^{***}P < 0.001$ vs. control (40% ethanol treated CER5/CHOL/PA bilayers) (Dunnett's test); $^{\#\#}P < 0.01$ vs. sample treated with *l*-menthol (Student's *t* test).

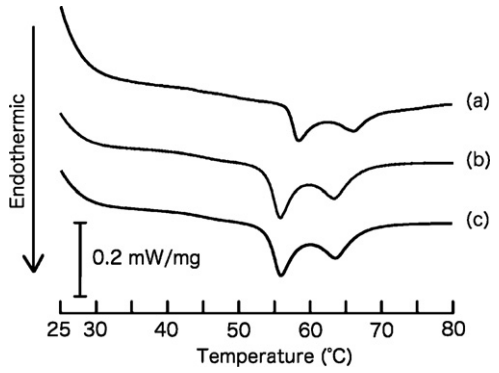

Fig. 2. DSC thermograms of CER5/CHOL/PA bilayers after treatment with optically active menthols. Menthols (10 mol%) relative to the total lipid of the bilayers were applied to the CER5/CHOL/PA bilayers for 2 h at 37 °C. The temperature was scanned at 10 °C/min. (a) Control, 40% ethanol treated CER5/CHOL/PA bilayers; bilayers after treatment with (b) *l*- and (c) *d*-menthols.

from the data of Fig. 2. The temperature of the first phase transition was shifted to a lower temperature, to 56.7 and 55.9 °C by treatment with 10 mol% *l*- and *d*-menthol, respectively (Fig. 3(a)). The transition enthalpy was reduced to the same extent by treatment with 10 mol% *l*- and *d*-menthol, to 0.899 and 1.10 mJ/mg, respectively (Fig. 3(b)). Only *d*-menthol significantly reduced the second phase transition temperature to 63.7 °C and the enthalpy to 3.034 mJ/mg.

We then separated the DRMs from the CER5/CHOL/PA bilayers by incubation with TX-100. As shown in Table 1, the molar ratios of CER5, CHOL, and PA in the DRMs were 40.8 ± 2.8 mol%, 26.5 ± 1.2 mol%, and 32.5 ± 1.6 mol%, respectively. The contents of CER5 and CHOL in the DRMs were increased almost twofold compared with those in the intact CER5/CHOL/PA bilayers. Fig. 4 shows the detergent insolubility after treatment with *l*- and *d*-menthols. The detergent insolubility decreased progressively, compared with the control level of 0.610, as *d*-menthol increased. In contrast, no significant effect was observed after treatment with *l*-menthol.

Table 1
The molar ratios of CER5, CHOL, and PA in DRMs.

	CER5 (mol%)	CHOL (mol%)	PA (mol%)
CER5/CHOL/PA bilayers	26.5	13.9	59.6
DRMs	40.8 ± 2.8	26.5 ± 1.2	32.5 ± 1.6

Each value represents a mean ± S.D. ($n = 3$).

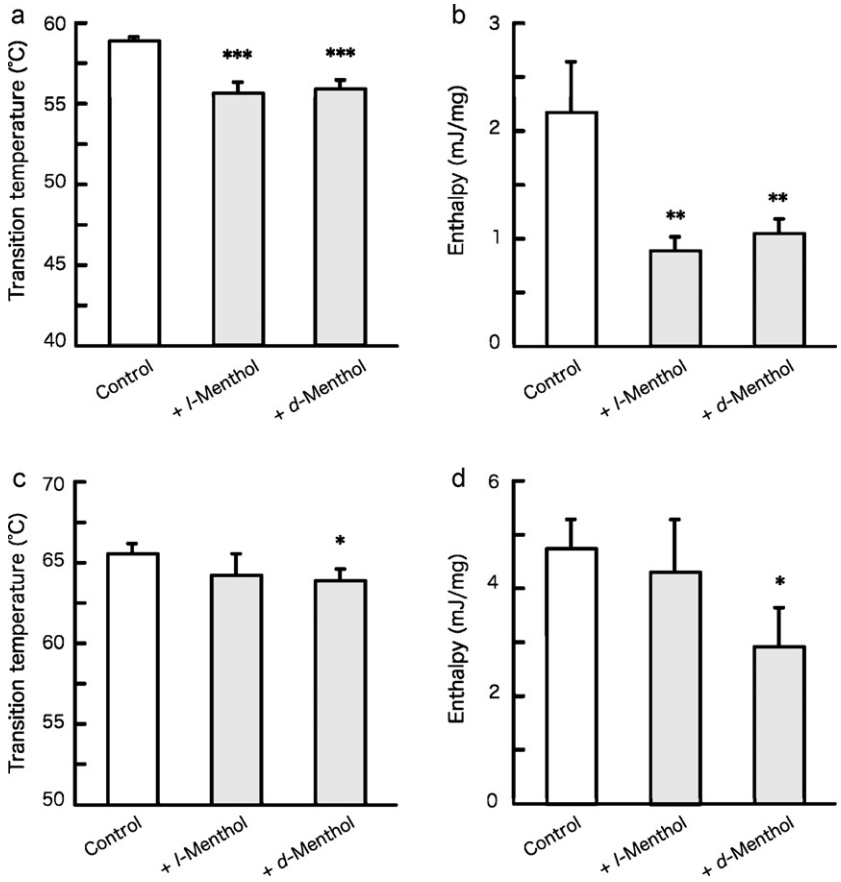

Fig. 3. Changes in the thermodynamic parameters of CER5/CHOL/PA bilayers. The phase transition temperature (a and c) and transition enthalpy (b and d) for the first peak (a and b) and the second peak (c and d) were calculated from the DSC curves shown in Fig. 2. Each column represents a mean ± S.D. ($n = 3$). $^{*}P < 0.05$, $^{**}P < 0.01$ and $^{***}P < 0.001$ vs. control (40% ethanol treated CER5/CHOL/PA bilayers) (Dunnett's test).

3.2. *Effects of the optical activity of menthols on the hydrocarbon chain packing of CER5/CHOL/PA bilayers examined by WAXS*

The effects of optically active menthols on hydrocarbon chain packing were investigated using WAXS. Fig. 5 shows the WAXS profiles for CER5/CHOL/PA bilayers treated with 10 mol% *l*- and *d*-menthol. Two diffraction peaks ($S = 2.39$ and $2.66\ \mathrm{nm}^{-1}$, corresponding to lateral distances of 0.418 and 0.376 nm, respectively) were obtained for the intact CER5/CHOL/PA bilayers. The integrated intensities of the diffraction peaks at $S = 2.39$ and $2.66\ \mathrm{nm}^{-1}$ were reduced and their peaks were shifted to lower lattice constants by 10 mol% *l*- and *d*-menthol. To clarify the effects of the optically active menthols on the hydrocarbon chain packing in the CER5/CHOL/PA bilayers, the apparent ratios of hydrocarbon chain packing (the $R_{\mathrm{Hexa/Ortho}}$ values) were calculated (Fig. 6). The $R_{\mathrm{Hexa/Ortho}}$ value was significantly increased by treatment with 10 mol% *l*-menthol, indicating that the relative amount of orthorhombic hydrocarbon chain packing was reduced from 41.3%

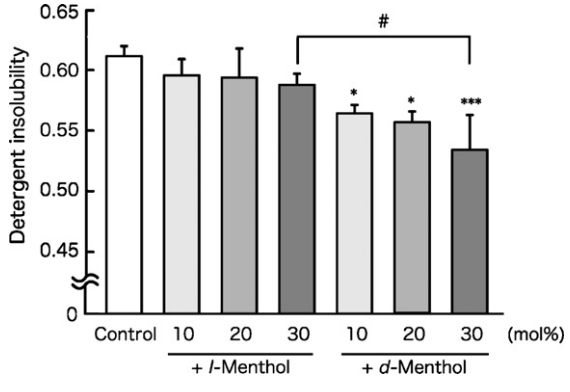

Fig. 4. Detergent insolubility of CER5/CHOL/PA bilayers. DRMs were extracted from the CER5/CHOL/PA bilayers by applying TX-100 to the CER5/CHOL/PA bilayer solution for 2 h at 25 °C. Each column represents a mean ± S.D. ($n = 3$). $^{*}P < 0.05$, $^{**}P < 0.01$ and $^{***}P < 0.001$ vs. control (40% ethanol treated CER5/CHOL/PA bilayers) (Dunnett's test); $^{\#}P < 0.05$ vs. sample treated with *l*-menthol (Student's *t* test).

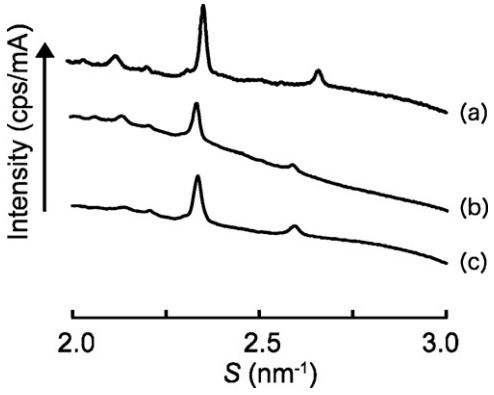

Fig. 5. SXRS profiles of CER5/CHOL/PA bilayers. Menthols (10 mol%) relative to the total lipid of the bilayers were applied to the CER5/CHOL/PA bilayers for 2 h at 37 °C. The temperature was scanned at 10 °C/min. (a) Control, 40%-ethanol-treated CER5/CHOL/PA bilayers; bilayers after treatment with (b) *l*- and (c) *d*-menthols. The reciprocal spacing is indicated by the formula: $S = n\lambda/2\sin\theta$, where λ is the wavelength of the X-ray, n is the degree of scattering, and θ is the scattering angle.

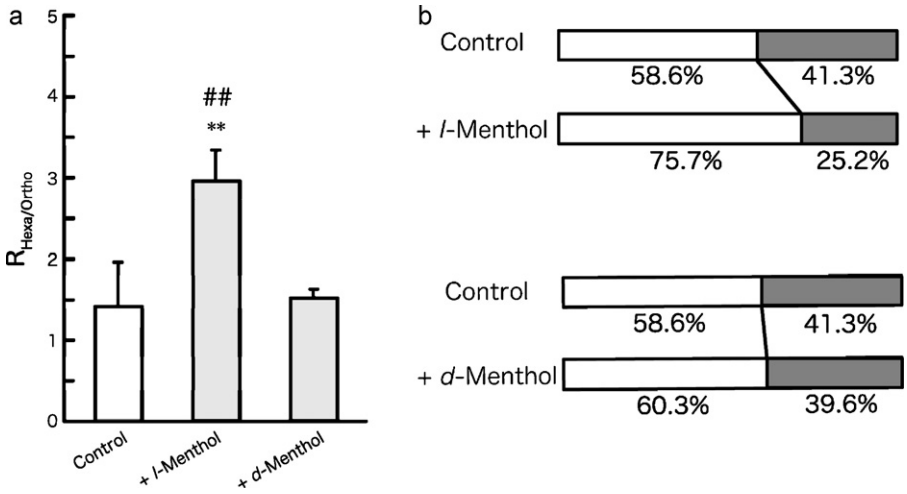

Fig. 6. Apparent ratio of hexagonal and orthorhombic hydrocarbon chain packing in CER5/CHOL/PA bilayers. (a) $R_{Hexa/Ortho}$ values were calculated from the analysis of the data in Fig. 5 using Eq. (2). Each column represents the mean ± S.D. ($n = 3$). $^{*}P < 0.05$ vs. control (40% ethanol treated CER5/CHOL/PA bilayers) and $^{\#\#}P < 0.01$ vs. sample treated with *d*-menthol (Dunnett's test). (b) Areas occupied by hexagonal and orthorhombic hydrocarbon chain packing were estimated based on the $R_{Hexa/Ortho}$ values. The opened and closed bars represent hexagonal and orthorhombic hydrocarbon chain packing, respectively. The method of estimating each type of packing was fully described in a previous study (Watanabe et al., 2010).

to 25.2%. In contrast, the $R_{Hexa/Ortho}$ value for the CER5/CHOL/PA bilayers was not altered by *d*-menthol.

4. Discussion

We investigated the effects of *l*- and *d*-menthol on CER5/CHOL/PA bilayers to estimate the difference their promoting activities in the transdermal drug permeation. Model membranes are effective for investigating the details of membrane changes, because the composition of a model membrane can be manipulated completely to suit the purpose of the experiment, and the findings are likely to be consistent. For the model membrane used in this study, simple components and a structure similar to that of biological membranes were required. The CER5/CHOL/PA bilayers were previously confirmed to be similar to the stratum corneum in terms of their lamellar structure and hydrocarbon chain packing (Watanabe et al., 2010).

We first examined the fluidizing effects of menthol with fluorescence anisotropy and DSC measurements. As shown in Fig. 1, treatment with optically active menthols induced the fluidization of the CER5/CHOL/PA bilayers. The effect of *d*-menthol was especially marked. From DSC measurements, the different effects of *l*- and *d*-menthols on the two main endothermic phase transitions of the CER5/CHOL/PA bilayers were examined (Figs. 2 and 3). The two optically active menthols acted equally on the first phase transition, whereas the second phase transition was only affected by *d*-menthol. Therefore, the fluidizing effect of *d*-menthol is stronger than that *l*-menthol. According to Kim et al. (1993) and Maghraby et al. (2005), the phase transition at about 58.6 °C represents the phase transition from the gel phase to the liquid-crystalline phase, and the phase transition at about 65.8 °C represents the conformational disorder of the liquid-ordered phase, as in membranes. Taken together, these findings suggest that *l*- and *d*-menthols have different modes of action on lipid bilayers.

In general, lipid bilayers are classified into three different phases in order of increasing fluidity: the solid-ordered phase, the liquid-disordered phase, and the liquid-ordered phase. Hydrocarbon chain packing in the solid-ordered phase is ordered and tight, whereas that in the liquid-disordered phase shows high lateral fluidity. CHOL-rich bilayers exist in the liquid-ordered phase, which is intermediate between the solid-ordered phase and the liquid-disordered phase. Its ordered hydrocarbon chain packing is similar to that of the solid-ordered phase, but its high lateral mobility is more similar to that of the liquid-disordered phase. The CER5/CHOL/PA bilayers in the cluster 2 might be formed the solid-ordered phase and liquid-ordered phase membranes at room temperature (Watanabe et al., 2010). Furthermore, Garibel et al. proposed that domain mosaic model as a model for the intercellular lipid in stratum corneum (Garibel et al., 2010). They suggested that intercellular lipid in stratum corneum is not homogenous structure so that means the distinct ordered phase is embedded in a more fluid liquid-ordered phase membrane. The variety of the microstructure may reflect the barrier function of the stratum corneum.

To investigate the effects of optically active menthols on ordered phase membranes, we conducted a detergent insolubility study of the CER5/CHOL/PA bilayers. This method is based on the observation that ordered lipid domains tend to resist solubilization by nonionic detergents, such as TX-100, whereas disordered fluid domains dissolve in these detergents. The insoluble membrane fraction, DRM, has been used as an index of the tightly packed domains that are present in samples before the addition of the detergent (Wang et al., 2004; Onuki et al., 2008).

We initially characterized the DRMs extracted from the CER5/CHOL/PA bilayers. From quantitative determination of the lipid composition, the molar fraction of CER5 and CHOL in DRMs were strongly increased. In the case of amount of CHOL, a large number of CHOL was excited in the DRMs. These indicated that DRMs are CHOL-rich membranes (Table 1). In a range of temperature from 50.0 to 70.0 °C, there was no marked reduction in the values representing the phase transitions, and the values were high enough to regard the DRMs as ordered-phase membranes (also see Supplemental data, Fig. S1). Intact CER5/CHOL/PA bilayers have a phase transition at about 60.0 °C, with a substantial reduction in the fluorescence anisotropy values, from 0.318 to 0.198 (Watanabe et al., 2010). Therefore, the DRMs obtained from the CER5/CHOL/PA bilayers were mostly composed of liquid-ordered phase membrane domains distributed in the membrane before TX-100 treatment. We then investigated the effects of optically active menthols on the DRMs. The DRMs were disturbed by the *d*-menthol treatment but resisted to the *l*-menthol treatment (Fig. 4), suggesting that the liquid-ordered phase membranes were changed into disordered phase membranes by treatment with *d*-menthol.

We further examined the effects of *l*- and *d*-menthols on the hydrocarbon chain packing in the CER5/CHOL/PA bilayers using WAXS. SXRS analyses have offered significant insight into the microstructure of the stratum corneum, including its lamellar structure and lateral hydrocarbon chain packing (Obata et al., 2006a,b). There are two lines of microstructures in the lamellar structure. One of them is a short lamellar structure with a repeat distance of about 6 nm, and the other is a long lamellar structure with a repeat distance thought to be about 13 nm (Bouwstra et al., 1991; Charalambopoulou et al., 2004). The type of hydrocarbon chain packing is distinguished in terms of lattice constants; i.e., a single peak at 0.24 nm^{-1} represents hexagonal hydrocarbon chain packing and peaks at 0.24 and 0.27 nm^{-1} represent orthorhombic hydrocarbon chain packing (Bouwstra et al., 1992). The WAXS profiles of the intact CER5/CHOL/PA bilayers showed two kinds of distinctive diffraction peaks (Fig. 5(a)). These diffractions indicate that the CER5/CHOL/PA bilayers were organized with hexagonal and orthorhombic hydrocarbon chain packing similar to the intercellular lipids in the human stratum corneum (Watanabe et al., 2010). The integrated intensities of the diffraction peaks for the CER5/CHOL/PA bilayers at $S = 2.39$ and 2.66 nm^{-1} were reduced by treatment with *l*- or *d*-menthol. Furthermore, the positions of both peaks were shifted to lower lattice constants. These results indicate that the menthols disturbed the tightly packed hydrocarbon chains in the CER5/CHOL/PA bilayers. We also calculated the $R_{Hexa/Ortho}$ values after treatment with the optically active menthols. Treatment with *l*-menthol significantly increased the $R_{Hexa/Ortho}$ value, representing a reduction in the orthorhombic hydrocarbon chain packing in the CER5/CHOL/PA bilayers, with high specificity (Fig. 6). By contrast, *d*-menthol treatment did not alter the $R_{Hexa/Ortho}$ value, so there was no effect on the apparent ratio between the hexagonal and orthorhombic hydrocarbon chain packing. These indicated the *l*-menthol specifically interacts with orthorhombic hydrocarbon chain packing, whereas *d*-menthol allows the fluidization of whole membrane, regardless of its membrane properties.

Different effects of *l*- and *d*-menthols on the CER5/CHOL/PA bilayers were inferred from these findings. A possible explanation is that *l*-menthol recognizes the chiral positions of the lipid bilayers. Among the components of the CER5/CHOL/PA bilayers, CER5 has optical activity that similar to the nature intercellular lipid in stratum corneum. Therefore, *l*-menthol partitions negligibly to CER5-rich microstructures, which exist as hexagonal hydrocarbon chain packing, and then fluidizes them with high selectivity. We think it is possible that the highly specific effect of *l*-menthol on the lipid bilayer plays an important role in its enhancement of transdermal drug permeation.

In conclusions, our CER5/CHOL/PA bilayers are useful tools for identifying the functions of the intercellular lipids in the stratum corneum and the mechanisms responsible for the effects of permeation enhancers, such as *l*-menthol. Using these bilayers, we clarified the distinct effects of *l*- and *d*-menthols on CER5/CHOL/PA bilayers. The action of *l*-menthol on CER5/CHOL/PA bilayers was highly specific compared with that of *d*-menthol; *l*-menthol acted negligibly on the liquid-ordered phase membrane and hexagonal hydrocarbon chain packing. The distinct effects obtained in this study may well be associated with the permeation enhancing effects of optically active menthols. But detailed effect of optically active menthols on the intrinsic intercellular lipids did not fully clarified yet. Further effort should be paid to clarify the mode of action of menthols on the intercellular lipids in stratum corneum.

Acknowledgments

The SXRS experiments were performed in a BL15A at the Photon Factory with the approval of the Photon Factory Advisory Committee (2008G079 and 2010G096) and BL40B2 of SPring-8 under the Priority Nanotechnology Support Program administered by the Japan Synchrotron Radiation Research Institute (JASRI) (Proposal No. 2010A1653). This work was supported by a grant from the Ministry of Education, Culture, Sports, Science and Technology of Japan. We would also like to express our gratitude and deepest appreciation to Prof. Hiroshi Takahashi (Gunma University, Department of Biological and Chemical Engineering, Gunma, Japan), Prof. Satoru Kato, and Dr. Masanao Kinoshita (Kwansei Gakuin University, Department of Physics, Hyogo, Japan) for their assistance with the WAXS measurements and their valuable advice.

Appendix A. Supplementary data

Supplementary data associated with this article can be found, in the online version, at doi:10.1016/j.ijpharm.2010.09.038.

References

Amit, K.J., Narisatty, S.T., Ramesh, P., 2002. Transdermal drug delivery of imipramine hydrochloride. I. Effect of terpenes. J. Control. Release 79, 93–101.
dos Anjos, J.L.V., Alonso, A., 2008. Terpenes increase the partitioning and molecular dynamics of an amphipathic spin label in stratum corneum membranes. Int. J. Pharm. 350, 103–112.
dos Anjos, J.L.V., Neto, D.S., Alonso, A., 2007. Effects of ethanol/*l*-menthol on the dynamics and partitioning of spin-labeled lipids in the stratum corneum. Eur. J. Pharm. Biopharm. 67, 406–412.
Barry, B.W., 1991. Lipid-protein-partitioning theory of skin permeation enhancement. J. Control. Release 15, 237–248.
Bouwstra, J.A., Gooris, G.S., van der Spek, J.A., Bras, W., 1991. Structural investigations of human stratum corneum by small-angle X-ray scattering. J. Invest. Dermatol. 97, 1005–1012.
Bouwstra, J.A., Gooris, G.S., Salomone-de Vries, M.A., van der Spek, J.A., Bras, W., 1992. Structure of human stratum corneum as a function of temperature and hydration: a wide-angle X-ray diffraction study. Int. J. Pharm. 84, 205–216.
Bouwstra, J.A., Gooris, G.S., Dubbelaar, F.E.R., Ponce, M., 2002. Phase behavior of stratum corneum lipid mixture based on human ceramides: the roke of natural and synthetic ceramide 1. J. Invest. Dermatol. 118, 606–617.
Charalambopoulou, G.C., Steriotis, T.A., Hauss, T., Stubos, A.K., Kanclloupoulos, N.K., 2004. Structural alterations of fully hydrated human stratum corneum. Physica B, e603–e606.
Emmanuella, C.G., Ali, T., Cecile, L., Arletta, B.G., 2009. Molecular interaction of penetration enhancers within ceramide organization: a FTIR approach. Eur. J. Pharm. Sci. 36, 192–199.
Garibel, K., Folting, B., Schaller, I., Kerth, A., 2010. The microstructure of the stratum corneum lipid barrier: mid-infrared spectroscopic studies of hydrated ceramide:palmitic acid:cholesterol medel systems. Biophys. Chem. 150, 144–156.
Groen, D., Gooris, G.D., Bouwstra, J.A., 2010. Model membranes prepared with ceramide EOS, cholesterol and free fatty acids form a unique lamellar phase. Langmuir 26, 4168–4175.
Kaliam, Y.N., Naik, A., Garrison, J., Guy, R.H., 2004. Iontophoretic drug delivery. Adv. Drug Deliv. Rev. 56, 619–658.
Kim, C.K., Hong, M.S., Kim, Y.B., Han, S.K., 1993. Effect of penetration enhancers (pyrrolidone derivatives) on multilamellar liposomes of stratum corneum lipid: a study by UV spectroscopy and differential scanning calorimetry. Int. J. Pharm. 95, 43–50.
Mackay, K.M.B., Williams, A.C., Barry, B.W., 2001. Effect of melting point of chiral terpenes on human stratum corneum uptake. Int. J. Pharm. 228, 89–97.
Maghraby, G.M.M.E., Campbell, M., Finnin, B.C., 2005. Mechanisms of action of novel skin penetration enhances. Phospholipid versus skin lipid liposomes. Int. J. Pharm. 305, 90–104.
Mohammed, A., Abdul, A., Yasumin, S., Asgar, A., 2007. Status of terpenes as skin penetration enhancers. Drug Discov. Today 12, 1061–1067.
Nakamura, Y., Takayama, K., Higashiyama, K., Suzuki, T., Nagai, T., 1996. Promoting effect of *O*-ethylmenthol on the percutaneous absorption of ketoprofen. Int. J. Pharm. 145, 29–36.
Narishetty, S.T.K., Panchagnula, R., 2005. Effect of *l*-menthol and 1,8-cineole on phase behavior and molecular organization of SC lipid and skin permeation of zidovudine. J. Control. Release 102, 59–70.
Obata, Y., Utsumi, S., Watanabe, H., Suda, M., Tokudome, Y., Otsuka, M., Takakyama, K., 2010. Infrared spectroscopic study of lipid interaction in stratum corneum treated with trandermal absorption enhancers. Int. J. Pharm. 389, 18–23.
Obata, Y., Hatta, I., Ohta, N., Kunizawa, N., Yagi, N., Takayama, K., 2006a. Combined effects of ethanol and *l*-menthol on the hairless rat stratum corneum investigated by synchrotron X-ray diffraction. J. Control. Release 115, 275–279.
Obata, Y., Maruyama, Y., Takayama, K., 2006b. The mode of promoting activity of *O*-ethylmethanol as a transdermal absorption enhancer. Pharm. Res. 23, 392–400.

Obata, Y., Takayama, K., Maitani, Y., Machida, Y., Nagai, T., 1993. Effect of pretreatment with skin with cyclic monoterpenes on permeation of diclofenac in hairless rat. Biol. Pharm. Bull. 16, 312–314.

Onuki, Y., Hagihara, C., Sugibayashi, K., Takayama, K., 2008. Specific effect of polyunsaturated fatty acids on the cholesterol-poor membrane domain in a model membrane. Chem. Pharm. Bull. 56, 1103–1109.

Prausnitz, M.R., 2004. Microneedles for transdermal drug delivery. Adv. Drug Deliv. Rev. 56, 581–587.

Suhonen, M., Li, S.K., Higuchi, W.I., Herron, J.N., 2008. A liposome permeability model for stratum corneum lipid bilayers based on commercial lipid. J. Pharm. Sci. 97, 4278–4293.

Kommura, T.R., Khan, M.A., Reddy, I.K., 1998. Racemate and enantiomers of ketoprofen: phase diagram thermodynamic studies, skin permeability, and use of chiral permeation enhancers. J. Pharm. Sci. 87, 833–840.

Wang, J., Megha, London, E., 2004. Relationship between sterol/steroid structure and participation in ordered lipid domains (lipid rafts): implications for lipid raft structure and function. Biochemistry 43, 1010–1018.

Watanabe, H., Obata, Y., Ishida, K., Takayama, K., 2009. Effect of *l*-menthol on the thermotropic behavior of ceramide 2/cholesterol mixture as a model for the intercellular lipids in stratum corneum. Colloids Surf. B 73, 116–121.

Watanabe, H., Obata, Y., Onuki, Y., Ishida, K., Takayama, K., 2010. Novel preparation of intercellular lipid models of the stratum corneum containing steroactive ceramide. Chem. Pharm. Bull. 58, 312–317.

Wertz, P.W., Abraham, W., Landmann, L., Downing, D.T., 1986. Preparation of liposomes from stratum corneum lipids. J. Invest. Dermatol. 87, 582–584.

Zhang, C.F., Yang, Z.L., Luo, J.B., 2006. Effect of enantiomer and isomer permeation enhancers on transdermal delivery of ligustrazine hydrochloride. Pharm. Dev. Technol. 11, 417–424.